

SCIENTIFIC REPORTS



OPEN

Evidence for a bi-partition of the Younger Dryas Stadial in East Asia associated with inversed climate characteristics compared to Europe

Received: 03 August 2016
Accepted: 17 February 2017
Published: 31 March 2017

Gordon Scholaut^{1,2}, Achim Brauer², Takeshi Nakagawa^{3,4}, Henry F. Lamb⁵, Jonathan J. Tyler⁶, Richard A. Staff^{7,†}, Michael H. Marshall⁵, Christopher Bronk Ramsey⁷, Charlotte L. Bryant⁸ & Pavel E. Tarasov⁹

The Younger Dryas Stadial (YDS) was an episode of northern hemispheric cooling which occurred within the Last Glacial Interglacial Transition (LGIT). A major driver for the YDS climate was a weakening of the Atlantic Meridional Overturning Circulation (AMOC). It has been inferred that the AMOC began to strengthen mid-YDS, producing a bipartite structure of the YDS in records from continental Europe. These records imply that the polar front and westerlies shifted northward, producing a warmer second phase of the YDS in Europe. Here we present multi-proxy data from the sediments of Lake Suigetsu (Japan), as evidence that a related bi-partition of the YDS also occurred in East Asia. Besides showing for the first time that the bi-partition was not limited to the North Atlantic/European region, the data also imply a climatic dipole between Europe and East Asia since the cold-warm characteristics are reversed at Lake Suigetsu. We suggest that changes in eastward moisture transport from the North Atlantic are the primary mechanism by which the teleconnection can be explained.

The Younger Dryas Stadial (YDS) occurred between ≈ 12.8 and ≈ 11.6 ka BP and while the exact mechanisms behind the YDS remain enigmatic^{1–3}, it is known that a weakening of the Atlantic Meridional Overturning Circulation (AMOC) occurred during this interval⁴, which was a strong driver for the YDS climate. Recent studies show that the AMOC regained some of its strength mid-YDS^{5–7}, resulting in a northward shift of the oceanic polar front starting at about 12.3 ka BP⁷. Associated with this shift was an increase in the variability of sea ice cover, due to a negative feedback system between AMOC changes and sea ice extent⁵ resulting in unstable climatic conditions. This climatic change produced a bi-partition of the YDS in European records^{5,8–10}. For instance, at Lake Kråkenes (Norway), a sudden climatic shift occurred at about 12.15 ka BP, indicating a northward shift of the atmospheric polar front and the westerlies as well as unstable climatic conditions⁵. Furthermore, through linking Lake Kråkenes with Meerfelder Maar (MFM) (Germany), using the Vedde ash as an isochron between the two archives, it was shown that the bi-partition of the YDS occurred earlier in more southerly regions; i.e. that the climatic change was time transgressive from south to north, reflecting the northward shift of the atmospheric polar front⁹. At MFM the bi-partition is recorded at 12.24 ka BP as a sudden increase in spring snowmelt from one year to the next⁹. The climatic change associated with the bi-partition also affected the dust flux in the Greenland

¹Centre for Ocean Drilling Science (ODS), Japan Agency for Marine-Earth Science and Technology (JAMSTEC), 3173-25 Showa-machi, Kanazawa-ku, Yokohama, 236-0001 Japan. ²Section 5.2: Climate Dynamics and Landscape Evolution, GFZ German Research Centre for Geosciences, Telegrafenberg, 14473 Potsdam, Germany. ³Research Centre for Palaeoclimatology, Ritsumeikan University, 1-1-1 Noji-Higashi, Kusatsu, Shiga 525-8577, Japan. ⁴Department of Geography, University of Newcastle upon Tyne, Newcastle upon Tyne, NE1 7RU, UK. ⁵Department of Geography and Earth Sciences, Aberystwyth University, Aberystwyth SY23 3DB, UK. ⁶Department of Earth Sciences, University of Adelaide, South Australia 5005, Australia. ⁷Research Laboratory for Archaeology and the History of Art (RLAHA), University of Oxford, Oxford, OX1 3QY, UK. ⁸NERC Radiocarbon Facility (East Kilbride), Scottish Enterprise Technology Park, Rankine Avenue, East Kilbride, Scotland, G75 0QF, UK. ⁹Institute of Geological Sciences, Palaeontology Section, Free University Berlin, Malteserstr, 74-100, Haus D, 12249 Berlin, Germany. [†]Present address: SUERC, University of Glasgow, Scottish Enterprise Technology Park, Rankine Avenue, East Kilbride, Scotland G75 0QF, UK. Correspondence and requests for materials should be addressed to G.S. (email: gosch@jamstec.go.jp)

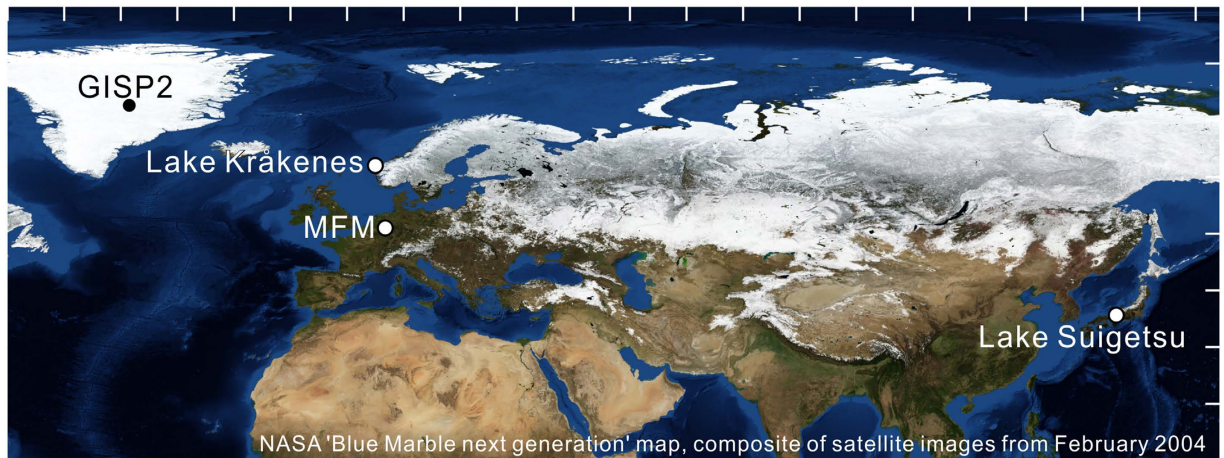


Figure 1. Location of Lake Suigetsu and sites referenced in the main text. Background map by NASA³⁵, latitude and longitude scale resolution is 10°.

ice cores^{9,11}, with higher values during the first phase of the YDS and lower values during the second, though the mechanism behind this change is uncertain⁹. The transition is not as distinct as in the other records due to a generally high variability, but occurred around 12.1 ka BP.

To investigate whether these North Atlantic changes also affected Asia, a climatically sensitive archive with a robust age model is required. Lake Suigetsu (Japan, 35°35'N, 135°53'E, 0 m above sea level, Fig. 1) represents such an archive in East Asia. It has previously been shown to record changes in the East Asian Monsoon (EAM) system including both the East Asian Winter Monsoon (EAWM) and the East Asian Summer Monsoon (EASM)¹². Furthermore, it has also been extensively dated¹³ and its chronology is a fundamental part of the IntCal13 radiocarbon calibration dataset¹⁴. The age model is based on a dual-method varve count^{15,16}, further constrained by speleothem derived U-Th ages that were modelled onto the varve chronology using the $\Delta^{14}\text{C}$ signals of the respective archives as a linkage¹³. The resulting chronology is denoted 'SG06₂₀₁₂ ka BP' with the year zero corresponding to A.D. 1950. The SG06₂₀₁₂ chronology enables an independent and precise comparison with the Greenland ice cores and with the MFM since the chronologies of these archives are also based on annual laminae counting. Issues with ¹⁴C dating, such as plateaus in the calibration curve, are thus avoided. For the study presented here, we used the continuous 'SG06' composite sediment core¹⁷. The position of the YDS in the SG06 sediment core was previously determined using pollen, microfacies and diatom data¹⁸. Combining the position of the YDS boundaries, originally published on a floating varve chronology, with the SG06₂₀₁₂ chronology, the YDS began at Lake Suigetsu at $12,780 \pm 31$ SG06₂₀₁₂ yr BP and terminated at $11,593 \pm 38$ SG06₂₀₁₂ yr BP. These ages mean that the YDS was synchronous within dating uncertainties between Suigetsu and the North Atlantic region.

For the study presented here, we conducted a high resolution, multi-proxy analysis of the YDS section of the Lake Suigetsu sediments. Microfacies analysis was applied^{16,19} and μXRF measurements were made with a 60 μm resolution¹⁵. Both methods provided data at sub-annual resolution. Continuous pollen analysis was carried out at 1 cm resolution (corresponding to about 12 years on average). The results of the pollen analysis were then translated into estimates of seasonal and annual temperature and precipitation using the modern analogue technique²⁰. $\delta^{15}\text{N}$ measurements on bulk sediment were made at low resolution (≈ 15 cm for the whole 73 m SG06 profile)²¹.

Results and Discussion

All of the employed techniques (microfacies, μXRF , pollen, and bulk isotope analysis) reveal a two-phase character of the YDS at Lake Suigetsu (Fig. 2). The age of the change in the individual proxies varies within the interval 12.22 to 12.01 ka SG06₂₀₁₂ BP (Table 1), indicating that the transition between the two YDS phases was coincident with, but not as sudden as at MFM or Lake Kråkenes; it occurred over a longer time frame in which the proxies reacted differentially to the climatic change.

The pollen-based temperature reconstruction shows declining temperatures with a high variability in the first part of the YDS and stable and cool conditions during the second part (Fig. 2a), with no distinguishable difference in character between seasonal and annual reconstructions (Supplementary Fig. S2). It has been shown (for orbital time scales) that temperature changes in Japan are strongly tied to glacial forcing²². Therefore the data suggest a southward shift of climate zones caused by an augmentation of the polar cell in the first part of the YDS and a steady state in the second part. The high variability during the first phase of the YDS indicates that the transport of cold polar air was frequently enhanced. In the present-day climate the development of the Okhotsk High can enhance the transport of polar air to northeastern Japan (known as Yamase winds)^{23,24}. We suggest that a similar, but geographically modified, mechanism was at work during the first phase of the YDS.

The observed cooling also led to a strengthening of the EAWM. The pollen-based precipitation reconstruction shows that winter (October to March) precipitation was enhanced during the YDS, with a further increase occurring in the second phase of the YDS (Fig. 2b), which also resulted in a clear increase in the mean annual precipitation (Fig. S2). These changes can be directly translated into a strengthening of the EAWM¹² and thus

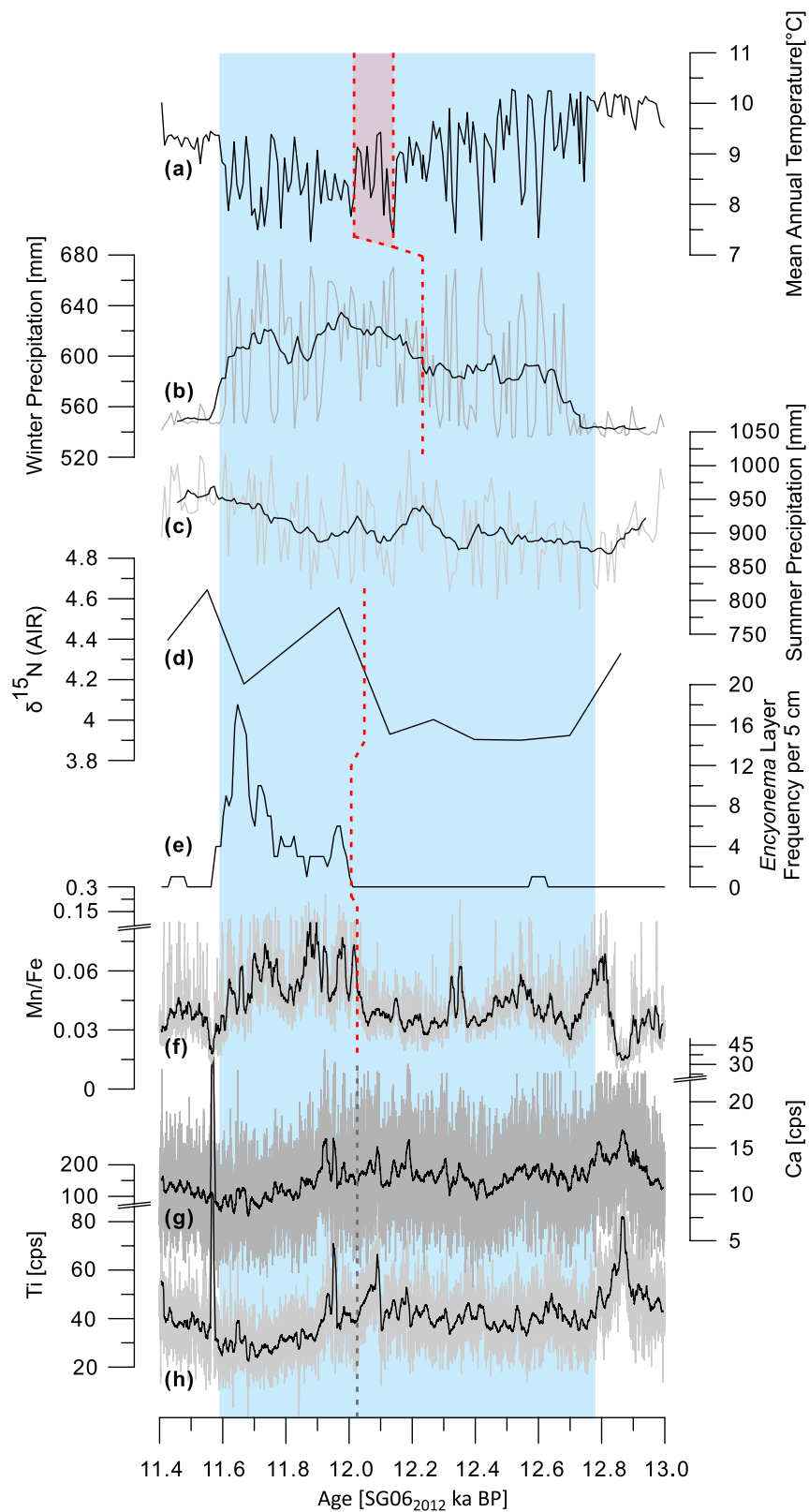


Figure 2. Summary of results from the multi-proxy analysis of the YDS interval of core SG06. In (b,c), and (f) to (h) grey curves are original data; black lines are the moving average ((b,c) 11 pt, (f) to (h) 201 pt); red dashed line marks the point of bi-partition in the respective proxies (see supplement for further details); in (g) and (h) the trend-signal is overprinted by event layers around the bi-partition, therefore, the point of change is uncertain and a grey dashed line (extrapolated from the Mn/Fe ratio) is used; note that the μ XRF curve of K is not shown since it is strongly correlated with Ti ($R=0.74$; Fig. S3); light blue background marks the YDS.

Proxy	mid YDS transition at	
	depth [cm cd]	age [SG 06 ₂₀₁₂ ka BP]
<i>Encyonema</i> layer frequency	1478.0 ± 0.1	12.01 ± 0.05
Mn and Mn/Fe (μ XRF)	1479.4 ± 0.1	12.02 ± 0.05
pollen based temperature reconstruction	1490.9–1478.7 ± 0.6	12.14–12.02 ± 0.06
visual microfacies analysis	1498.9 ± 0.1	12.22 ± 0.04
pollen based winter precipitation reconstruction	1499.0 ± 0.6	12.22 ± 0.05

Table 1. Position in composite depth (cd) and age of the bi-partition in the individual proxies analysed here. For boundary determination see Fig. 2 (more details are given in the supplement).

to a cooling of the Siberian/Mongolian air mass. Pollen and μ XRF element curves of Ti, K and Ca show that the EASM reacted inversely to the forcing. The pollen-based reconstruction of summer precipitation shows reduced values throughout the YDS (Fig. 2c), indicating a weakening of the summer (April to September) monsoon rainy season. Although the reconstructed summer precipitation does not show the bi-partition of the YDS, a decline in the μ XRF element curves of Ti, K and Ca occurs in the second part of the YDS (Fig. 2g,h; Fig. S3). The decline is moderate but statistically significant (Welsh-test yields: p-values < 2.2e-16 for all three elements; data affected by two detrital event layers occurring between 12.10 and 11.93 ka BP were excluded, populations are thus from 12.78–12.10 ka BP and 11.93–11.59 ka BP). The lower values suggest a further weakening of the summer monsoon rainy season in the second phase of the YDS. Since Ti, K and Ca are proxies for detrital inwash into the lake¹⁹; their decline is indicative of a decrease in catchment erosion and thus a reduction in precipitation (see supplement for further details). Precipitation at Lake Suigetsu is primarily due to the summer monsoon rainy season and to typhoons (Fig. S4). Since the reconstruction of the flood history at Lake Suigetsu shows that the typhoon frequency was reduced throughout the YDS¹⁹, the moderate decrease in Ti, K and Ca is likely to be due to a weakening of the EASM rainy season in the second part of the YDS. The pollen-based precipitation reconstruction may not be sensitive enough to record this moderate change, especially since the precipitation reconstruction has a higher degree of uncertainty than the temperature reconstruction²⁰.

Microfacies and stable isotope data suggest greater turbulence in the lake caused by increased wind stress during the second phase of the YDS. Figure 2d,e show that layers of *Encyonema* diatoms occur in the second part of the YDS and that $\delta^{15}\text{N}$ values are higher. Both proxies have previously been related to an increase in turbulence^{17,21} and no indications for diatom dissolution were found during the sediment analysis and therefore the data are not biased in this regard. Hence, the two proxies indicate an increase in wind stress. Greater wind stress is also inferred from the increased Mn/Fe ratio in the second part of the YDS, accompanied by enhanced siderite content (Fig. 2f; Fig. S6). In the case of Lake Suigetsu these changes indicate that the influx of Mn into the lake was increased (see supplement). Wave erosion of the shore as well as geochemical focusing of Mn in deeper parts of the lake due to resuspension of Mn-oxyhydroxides from shallower, oxic parts of the lake are likely explanations, considering that inwash into the lake was reduced as indicated by the μ XRF Ti, K and Ca data. We exclude a lake level lowering, which could produce a similar proxy response by increasing turbulence in previously deeper parts of the lake, because the increase in mean annual precipitation (Fig. S2) and the parallel decrease in temperature, and thus evaporation, make a lake level lowering unlikely. The greater wind stress was probably due to the strengthened EAWM and to migratory cyclones and anticyclones developing in spring, since these produce the highest mean monthly wind speeds in the present-day climate^{23,25}, and because typhoon frequency was reduced¹⁹. Both mechanisms, EAWM and migratory (anti) cyclones, are strongly tied to the temperature and pressure contrasts between the Siberian/Mongolian and the Pacific air masses and thus support the inference that the bi-partition of the YDS at Lake Suigetsu was brought about by a colder Siberian/Mongolian air mass in the second part of the YDS. However, whether the abrupt change in the Mn/Fe ratio and the *Encyonema* layer frequency is due to a sudden onset of stronger winds or the result of a threshold response to a gradual increase in wind strength over the transition interval remains uncertain.

The common timing of the bi-partition in European records, Greenland, and that of Lake Suigetsu (Fig. 3) suggests a link between the North Atlantic and Asian climatic changes. Changes in the westerlies and in North Atlantic sea surface temperatures (SST) are an important control on moisture in arid central Asia²⁶ from where the dust in Greenland is derived²⁷. The northward shift of the westerlies and the increased SSTs in the second phase of the YDS would have enhanced moisture transport towards central Asia. Thus, the reduced dust flux in Greenland^{9,11} (Fig. 2a) could be explained through an increased resistance to erosion in the source region as the result of higher moisture²⁸. The increased moisture transport would likely also have increased the snow cover in Eurasia. It has been shown that changes in snow cover over Eurasia generally²⁹ and over European Russia specifically³⁰ can influence atmospheric circulation and thus can lead to altered dust pathways in the atmosphere and/or increased rainout of dust. An increase in snow cover can also impact the monsoonal system, specifically strengthening the EAWM³¹ and weakening the EASM²⁹, in agreement with our reconstruction of the EAM. While the effect of snow cover is complex and has so far only been investigated in the present-day climate, it provides a likely explanation of how a strengthened AMOC could have reduced the dust flux to Greenland, produced a colder climate in East Asia, and thus led to the intercontinental bi-partition of the YDS and the climatic dipole between Europe and East Asia.

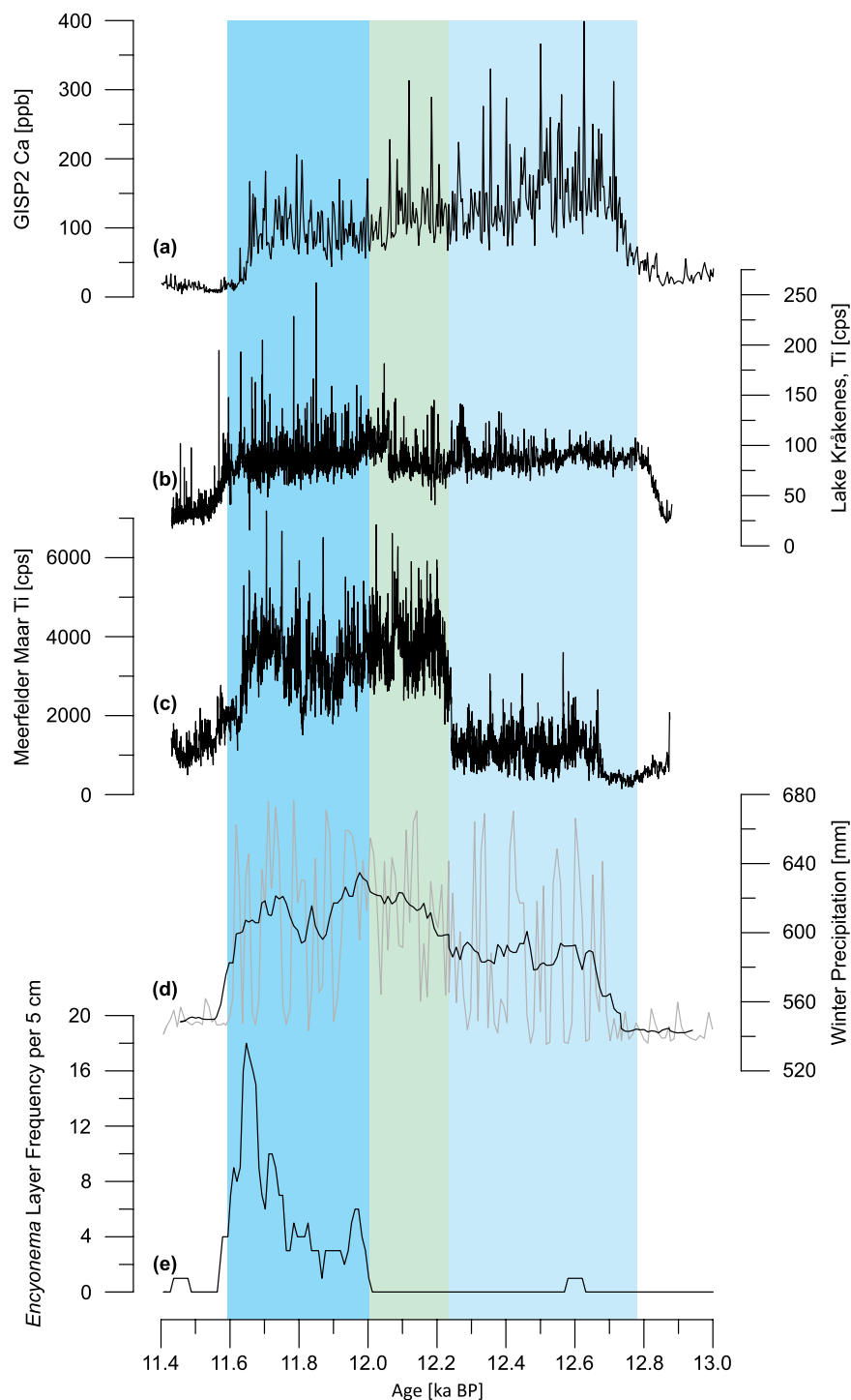


Figure 3. Comparison of (a) Greenland GISP2 dust record¹¹ (represented by Ca), (b) Ti record from Lake Kråkenes⁵ and (c) Ti record from MFM⁹ with (d,e) results from the study presented here; each plotted on their respective chronologies except (a) which is on the GICC05 time scale³⁶; background colours are with reference to Lake Suigetsu: light blue marks the first phase of the YDS, light green the transition interval and blue the second phase of the YDS.

Methods

Initial Sampling and Composite Model. The cores were split in the field and core photographs were taken under natural daylight and include a depth scale and a colour chart alongside the core. Based on the core photographs the composite model was created. The uncertainty of the composite depth is the standard reading error of 1 mm (i.e. one scale unit). Afterwards, the cores were sampled using LL-channels. The LL-channels were

then distributed for further analysis to the respective members of the 'Suigetsu Varves 2006' project. A detailed description of the coring and initial sampling can be found in ref. 17.

Microfacies Analysis. Microfacies analysis was based on visual evaluation of thin section scans¹⁹ and core photos. The thin section scans were made using a slide scanner with polarising foils. The resolution used was 1,200 dpi. Additionally, seasonal layer frequency data were generated through light microscopy. These data were measured using a petrographic microscope which was equipped with a calibrated ocular micrometer, using magnifications from 25× to 400×. Layer thickness and position measurements were made mainly at 25×. Therefore, the standard reading error is 0.04 mm.

μXRF Analysis. For μXRF analysis continuous measurements were made with an ITRAX core scanner on the sediment in LL-channels. For the Suigetsu sediment a 4 × 0.1 mm rectangular beam was used, with a step-size of 60 μm, a count time of 4 s, a voltage of 30 kV, a current of 30 mA and a Mo X-ray tube. A more detailed description of the settings used is given by¹⁵.

Pollen Analysis and Modern Analogue Technique. Samples were taken contiguously with 1 cm resolution and then treated by the method of³². Pollen grains were identified by light microscopy and counted until the sum of the 32 arboreal pollen taxa which were identified as the most representative of the vegetation and climate³³ exceeded 400 grains. Precision/stability of the pollen data were monitored by the standard sample method outlined by³⁴.

Pollen percentage data were converted into climate indices using the modern analogue method²⁰. Polygon software (<http://polsystems.rits-palaeo.com>) was used for calculations at the default setting of the software, i.e. number of modern analogues = 0 to 8, chord distance of threshold = 0.1; no enhancement of minor taxa. No data were rejected as outliers at this setting.

Nitrogen Isotope Analysis on Bulk Organic Matter. Cylindrical samples with a 1 cm diameter were taken with a ≈15 cm resolution. Dried sediments were powdered and acidified within Sn cups to remove carbonate traces. ¹⁵N/¹⁴N ratios were measured using a Fisons NA 1500 CHN analyser coupled to a Finnigan-MAT Delta Plus isotope ratio mass spectrometer. Isotope ratios were calibrated against histidine, in addition to an in-house standard (marine sediment), with a reproducibility of ±0.3‰. A more detailed description of this methodology is given by²¹.

References

- Bradley, R. S. & England, J. H. The Younger Dryas and the Sea of Ancient Ice. *Quaternary Res.* **70**, 1–10 (2008).
- Denton, G. H. *et al.* The Last Glacial Termination. *Science* **328**, 1652–1656 (2010).
- Renssen, H. *et al.* Multiple causes of the Younger Dryas cold period. *Nat. Geosci.* **8**, 946–950 (2015).
- McManus, J. F., Francois, R., Gherardi, J.-M., Keigwin, L. D. & Brown-Leger, S. Collapse and rapid resumption of Atlantic meridional circulation linked to deglacial climate changes. *Nature* **428**, 834–837 (2004).
- Bakke, J. *et al.* Rapid oceanic and atmospheric changes during the Younger Dryas cold period. *Nat. Geosci.* **2**, 202–205 (2009).
- Elmore, A. C. & Wright, J. D. North Atlantic Deep Water and climate variability during the Younger Dryas cold period. *Geology* **39**, 107–110 (2011).
- Pearce, C. *et al.* Ocean lead at the termination of the Younger Dryas cold spell. *Nat. Commun.* **4**, 1664, 10.1038/ncomms2686 (2013).
- Neugebauer, I. *et al.* A Younger Dryas varve chronology from the Rehwiess palaeolake record in NE-Germany. *Quaternary Sci. Rev.* **36**, 91–102 (2012).
- Lane, C. S., Brauer, A., Blockley, S. P. E. & Dulski, P. 2013. Volcanic ash reveals time-transgressive abrupt climate change during the Younger Dryas. *Geology* **41**, 1251–1254 (2013).
- Baldini, L. M. *et al.* Regional temperature, atmospheric circulation, and sea-ice variability within the Younger Dryas Event constrained using a speleothem from northern Iberia. *Earth Planet. Sci. Lett.* **419**, 101–110 (2015).
- Mayewski, P. A. *et al.* Major features and forcing of high-latitude northern hemisphere atmospheric circulation using a 110,000-year-long glaciochemical series. *J. Geophys. Res.* **102**, 26345–26366 (1997).
- Nakagawa, T., Tarasov, P. E., Kitagawa, H., Yasuda, Y. & Gotanda, K. Seasonally specific responses of the East Asian monsoon to deglacial climate changes. *Geology* **34**, 521–524 (2006).
- Bronk Ramsey, C. *et al.* A Complete Terrestrial Radiocarbon Record for 11.2 to 52.8 kyr B.P. *Science* **338**, 370–374 (2012).
- Reimer, P. *et al.* IntCal13 and Marine13 Radiocarbon Age Calibration Curves 0–50,000 Years cal BP. *Radiocarbon*. **55**, 1869–1887 (2013).
- Marshall, M. *et al.* A novel approach to varve counting using μXRF and X-radiography in combination with thin-section microscopy, applied to the Late Glacial chronology from Lake Suigetsu, Japan. *Quat. Geochronol.* **13**, 70–80 (2012).
- Schlolaut, G. *et al.* An automated method for varve interpolation and its application to the Late Glacial chronology from Lake Suigetsu, Japan. *Quat. Geochronol.* **13**, 52–69 (2012).
- Nakagawa, T. *et al.* SG06, a fully continuous and varved sediment core from Lake Suigetsu, Japan: stratigraphy and potential for improving the radiocarbon calibration model and understanding of late Quaternary climate changes. *Quaternary Sci. Rev.* **36**, 164–176 (2012).
- Kossler, A. *et al.* Onset and termination of the late-glacial climate reversal in the high-resolution diatom and sedimentary records from the annually laminated SG06 core from Lake Suigetsu, Japan. *Palaeogeogr. Palaeoclimatol. Palaeoecol.* **306**, 103–115 (2011).
- Schlolaut, G. *et al.* Event layers in the Japanese Lake Suigetsu 'SG06' sediment core: description, interpretation and climatic implications. *Quaternary Sci. Rev.* **83**, 157–170 (2014).
- Nakagawa, T., Tarasov, P. E., Nishida, K., Gotanda, K. & Yasuda, Y. Quantitative pollen-based climate reconstruction in central Japan: application to surface and Late Quaternary spectra. *Quaternary Sci. Rev.* **21**, 2099–2113 (2002).
- Tyler, J. *et al.* Tracking aquatic change using chlorine-specific carbon and nitrogen isotopes: The last glacial-interglacial transition at Lake Suigetsu, Japan. *Geochem. Geophys. Geosyst.* **11**, Q09010, 10.1029/2010GC003186 (2010).
- Nakagawa, T. *et al.* Regulation of the monsoon climate by two different orbital rhythms and forcing mechanisms. *Geology* **36**, 491–494 (2008).
- Japan Meteorological Agency, <http://www.jma.go.jp/jma/en/menu.html>.
- Kanno, H. Classification of the Yamase (Cold Northeasterly Wind around Northeastern Japan) Based upon its Air-Mass Vertical Structures. *J. Meteor. Soc. Japan* **75**, 1053–1071 (1997).

25. Takano, Y., Tachibana, Y. & Iwamoto, K. Influences of Large-scale Atmospheric Circulation and Local Sea Surface Temperature on Convective Activity over the Sea of Japan in December. *Sola* **4**, 113–116 (2008).
26. Chen, F. *et al.* Holocene moisture evolution in arid central Asia and its out-of-phase relationship with Asian monsoon history. *Quaternary Sci. Rev.* **27**, 351–364 (2008).
27. Bory, A. J.-M., Biscaye, P. E. & Grousset, F. E. Two distinct seasonal Asian source regions for mineral dust deposited in Greenland (NorthGRIP). *Geophys. Res. Lett.* **30**, 1167, 10.1029/2002GL016446 (2003).
28. Ruth, U., Wagenbach, D., Steffensen, J. P. & Bigler, M. Continuous record of microparticle concentration and size distribution in the central Greenland NGRIP ice core during the last glacial period. *J. Geophys. Res.* **108**, 4098; 10.1029/2002JD002376 (2003).
29. Barnett, T. P., Dümenil, L., Schlese, U. & Roeckner, E. The Effect of Eurasian Snow Cover on Global Climate. *Science* **239**, 504–507 (1988).
30. Ye, H. & Bao, Z. Lagged teleconnections between snow depth in northern Eurasia, rainfall in Southeast Asia and seas-surface temperatures over the tropical Pacific Ocean. *Int. J. Climatol.* **21**, 1607–1621 (2001).
31. Jhun, J.-G. & Lee, E.-J. A New East Asian Winter Monsoon Index and Associated Characteristics of the Winter Monsoon. *J. Clim.* **17**, 711–726 (2004).
32. Nakagawa, T., Brugiapaglia, E., Digerfeldt, G., Reille, M., Beaulieu, J.-L. & Yasuda, Y. Dense-media separation as a more efficient pollen extraction method for use with organic sediment/deposit samples: comparison with the conventional method. *Boreas* **27**, 15–24 (1998).
33. Gotanada, K., Nakagawa, T., Tarasov, P., Kitagawa, J., Inoue, Y. & Yasuda, Y. Biome classification from Japanese pollen data: application to modern-day and Late Quaternary samples. *Quaternary Sci. Rev.* **21**, 647–657 (2002).
34. Nakagawa, T., Kitagawa, H., Payne, R. & Tarasov, P. A standard sample method for controlling microfossil data precision: A proposal for higher data quality and greater opportunities for collaboration. *Quatern. Int.* **290–291**, 239–244 (2013).
35. Stöckli, R., Vermote, E., Saleous, N., Simmon R. & Herring, D. The Blue Marble Next Generation - A true color earth dataset including seasonal dynamics from MODIS. *NASA Earth Observatory* <http://earthobservatory.nasa.gov/Features/BlueMarble/bmgm.pdf> (2005).
36. Rasmussen, S. O. *et al.* A new Greenland ice core chronology for the last glacial termination. *J. Geophys. Res.* **111**, D06102, 10.1029/2005JD006079 (2006).

Acknowledgements

We thank the Japan Society for the Promotion of Science (JSPS KAKENHI grant JP15H06905, fellowship grant PE07622), the German Research Foundation (DFG grants BR 2208/7-1, TA-540/3-1, TA-540/5-2), the UK Natural Environment Research Council (NERC grants NE/D000289/1, NE/F003048/1, SM/1219.0407/001), and the Leverhulme Trust (grant ECF-2015-396).

Author Contributions

G.S.: microfacies analysis, μ XRF, chronology, development of original hypothesis. A.B.: microfacies analysis, chronology. T.N. and P.T.: pollen analysis, H.L. and M.M.: μ XRF, chronology. J.T.: stable isotope analysis. R.S., C.B.R. and C.B.: chronology all authors collaborated on the text.

Additional Information

Supplementary information accompanies this paper at <http://www.nature.com/srep>

Competing Interests: The authors declare no competing financial interests.

How to cite this article: Schlolaut, G. *et al.* Evidence for a bi-partition of the Younger Dryas Stadial in East Asia associated with inversed climate characteristics compared to Europe. *Sci. Rep.* **7**, 44983; doi: 10.1038/srep44983 (2017).

Publisher's note: Springer Nature remains neutral with regard to jurisdictional claims in published maps and institutional affiliations.



This work is licensed under a Creative Commons Attribution 4.0 International License. The images or other third party material in this article are included in the article's Creative Commons license, unless indicated otherwise in the credit line; if the material is not included under the Creative Commons license, users will need to obtain permission from the license holder to reproduce the material. To view a copy of this license, visit <http://creativecommons.org/licenses/by/4.0/>

© The Author(s) 2017